

9-27-2020

Experimental and model research on shear creep of granite under freeze-thaw cycles

Feng-rui ZHANG

An-nan JIANG
jiangannan@163.com

Xiu-rong YANG

FA -yi SHEN

Follow this and additional works at: <https://rocksoilmech.researchcommons.org/journal>



Part of the [Geotechnical Engineering Commons](#)

Custom Citation

ZHANG Feng-rui, JIANG An-nan, YANG Xiu-rong, SHEN FA -yi. Experimental and model research on shear creep of granite under freeze-thaw cycles[J]. Rock and Soil Mechanics, 2020, 41(2): 509-519.

This Article is brought to you for free and open access by Rock and Soil Mechanics. It has been accepted for inclusion in Rock and Soil Mechanics by an authorized editor of Rock and Soil Mechanics.

Experimental and model research on shear creep of granite under freeze-thaw cycles

ZHANG Feng-ruì, JIANG An-nan, YANG Xiu-rong, SHEN FA -yi

Institute of Road and Bridge Engineering, Dalian Maritime University, Dalian, Liaoning 116026, China

Abstract: To study the effect of freeze-thaw on the shear creep characteristics of engineering rocks in cold regions, the granite samples from Huibai tunnel in Jilin province were taken as the research object, and the microscopic characteristics and shear creep tests of samples under different freeze-thaw cycles were carried out. The results show that: 1) With the increase of freeze-thaw cycles, the cracks and voids in the samples develop continuously, and the damage of rock surface becomes more and more obvious. 2) The pores in the sample are mainly composed of small and medium pores, and the porosity increases nonlinearly with the increase of freeze-thaw cycles. 3) With the increase of freeze-thaw cycles, creep deformation and creep rate increase gradually, while creep time, failure stress and long-term strength decrease obviously. According to the test results, expressions of unsteady creep parameters of freeze-thaw rocks are established, the damage viscous element of freeze-thaw rock is proposed, and the freeze-thaw shear creep constitutive model of granite is constructed. By comparing creep test curve with theoretical model fitting curve, the correctness and applicability of the model are verified. Through sensitivity analysis of creep parameters, the influence of creep parameters on granite creep deformation is studied, and the variation law of creep parameters with the number of freeze-thaw cycles is given. The research results have guiding significance for long-term stability evaluation of rock mass engineering in cold regions.

Keywords: granite; freeze-thaw cycles; meso-damage; shear creep; experimental study; creep model

1 Introduction

The shear creep characteristic, which is closely related to the long-term stability of rock mass engineering, is one of the important mechanical characteristics of engineering rocks^[1]. In slope management, tunnel construction, and mining projects, the failure of rock mass due to long-term shear loading is one of its main failure mode. Especially with the development of rock mass engineering in cold regions, rock is severely deteriorated and damaged under freeze-thaw cycles, and shear creep characteristics are more significant, which will adversely affect the long-term stability of engineering in cold regions.

Scholars at home and abroad have carried out research on shear creep characteristics of rocks and achieved certain results. Jia et al. carried out shear creep tests of undisturbed rocks under different normal stresses and established an empirical formula for estimating creep strain^[2]. Zhao et al. studied the failure characteristics of red sandstone under shear creep, and analyzed the rock fracture surface based on micro-analysis technology and three-dimensional measurement device^[3]. Zhang et al. studied the shear creep characteristics of rocks through experiments and proposed a constitutive model that can reflect

the nonlinear creep characteristics of structural planes^[4]. Xu et al. studied the failure evolution characteristics of rocks through a series of shear creep tests on discontinuous rocks^[5]. Sun et al. carried out shear creep tests on rock masses with multiple groups of jointed and analyzed the rheological properties of the rocks^[6]. Wang et al. and Tian et al. carried out the shear creep test and model research of zigzag structural surface, and described the shear creep characteristics of zigzag structural surface.^[7–8] Xu et al. and Yang et al. established a nonlinear shear creep model based on the shear creep test results of mudstones from Longtan Hydropower Station^[9–10]. Li et al. carried out shear creep tests on sandstones with different moisture contents, and described the shear creep laws using Burgers model^[11]. Yu et al. established a nonlinear shear rheological model based on the nonlinear characteristics of creep of aqueous soft rocks^[12]. Liu et al. carried out shear rheological tests on tuff lava with different surrounding rock levels of the tunnel, and selected appropriate rheological models for fitting analysis based on the test curves^[13]. Fan et al. studied the shear creep characteristics of expansive rocks and obtained the fitting relationship between normal stress and long-term strength^[14]. Li et al. and Zhu et al. carried out shear

Received: 11 March 2019

Revised: 17 May 2019

This work was supported by the National Natural Science Foundation of China(51678101), the Central University Basic Research Fund Special Funds (3132014326) and the Jilin Province Transportation Project (2017ZDGC-2).

First author: ZHANG Feng-ruì, male, born in 1990, PhD candidate, majoring in stability analysis of geotechnical engineering. E-mail: zhangfengrui@dlmu.edu.cn

Corresponding author: JIANG An-nan, male, born in 1971, PhD, Professor, PhD supervisor, Research interests: geotechnical stability analysis and multi-field coupling. E-mail: jiangannan@163.com

creep tests on hard and weak structural surfaces of marble using biaxial creep meters, and proposed reasonable shear creep models. [15–16]

However, the existing researches on shear creep are mainly concentrated at room temperature, and there are few reports on the shear creep characteristics of rocks under freeze-thaw cycles. Shear creep processes in cold regions are mostly affected by freeze-thaw cycles, which exacerbate the damage and destruction of rocks and affect the creep characteristics of rocks.

Based on this, this study conducts meso-structure observations and shear creep tests on granite subjected to different freeze-thaw cycles, and analyzes the meso-damage and creep mechanism of granite under freeze-thaw cycles. Moreover, a freeze-thaw shear creep constitutive model of granite is constructed and verified with experimental data. The influence of creep parameters on the creep deformation of granite is studied through the sensitivity analysis, and the variation law of creep parameters with the number of freeze-thaw cycles is given. The research results have guiding significance for long-term stability evaluation of rock mass engineering in cold regions.

2 Experimental program

2.1 Specimen preparation

The specimens in this article were taken from the Huinan-Baishan Expressway Tunnel in Jilin province. They are gray-white granite. The main components are quartz, potassium feldspar and acid plagioclase. The minor minerals are biotite and amphibole. The rocks in the same tunnel face were selected on the site and brought back to the laboratory for high-precision cutting and smoothing. According to the requirements of the sample size in *Test Methods of Rock for Highway Engineering* (JTG E41—2005)^[17], the rock was processed into a 200 mm × 100 mm × 100 mm cube specimen, and then tested for porosity and wave velocity to select specimens with higher uniformity. Some of the produced specimens are shown in Fig. 1.



Fig.1 Granite sample

2.2 Experimental equipment and program

The freeze-thaw cycle tests used the high and low

temperature test chamber produced by Guangzhou Espek Company. This equipment can automatically control the cycle time and freezing and thawing temperature, with a temperature range of $-70-150\text{ }^{\circ}\text{C}$. The shear creep tests used the JAW-600 multifunctional shear rheometer produced by Changchun Chaoyang Testing Machine Factory, which is mainly composed of a shear loading system, a normal loading system, a shear box and a data acquisition system. This equipment can be used to perform the rock shear and shear creep tests. The maximum normal load and the maximum shear load of the equipment are 2 000 kN and 600 kN, respectively, and the measuring range of deformation is 0–20 mm (see Fig. 2).



Fig.2 JAW-600 multifunctional shear rheometer

Firstly, the rock specimens were saturated by vacuum extraction for 24 h, the saturated specimens were placed in a container containing water and then placed in a high and low temperature test box for freeze-thaw cycles, each cycle period is 24 h (12 hours at $-20\text{ }^{\circ}\text{C}$ and 12 hours at $20\text{ }^{\circ}\text{C}$). The specimens were subjected to 0, 10, 30, 50 and 70 freeze-thaw cycles, respectively. In order to minimize the influence of the differences of the specimens themselves, three granitic specimens were prepared for each number of freeze-thaw cycles, which means 15 specimens should be prepared.

In order to reveal the effect of freeze-thaw cycles on the microstructure of granite, SEM and NMR experiments were performed. The SEM equipment is shown in Fig. 3.



Fig.3 Scanning electron microscope equipment

After completing the corresponding number of freeze-thaw cycles, the specimens were removed for shear creep tests. During the test, the specimens were located between the upper and lower shear boxes, and the lower shear box was fixed on

the horizontal guide of the testing machine. The shear load was applied to the upper shear box by the shear loading system, in the meanwhile, the lower shear box also received forces with the same magnitude and opposite direction through the reaction force device. The normal load was applied to the upper shear box by the normal loading system. The vertical axis of the specimen coincided with the normal axis of the normal indenter, and the horizontal axis of the specimen was located at the middle of the upper and lower shear boxes. Figure 4 is a diagram of the shear creep test.

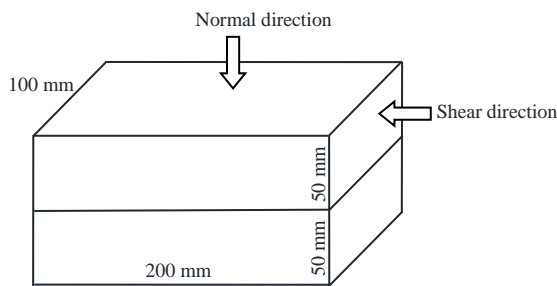


Fig.4 Shear creep diagram

The normal stress was determined as 5 MPa based on the average value of ground stress horizontal measurement of the tunnel surrounding rock. The total shear load was estimated according to 90% of the instantaneous shear strength of the test specimen, and the shear creep tests were performed at 4–6 stress levels. During the test, the initial shear stress and loading rate were set to be 2 MPa and 0.5 MPa/min, respectively. Until the specimen suffered shear failure, the next-stage shear load ($\Delta\tau=2$ MPa) was applied when the shear deformation rate was less than 5×10^{-4} mm/d. The test scheme is shown in Table 1.

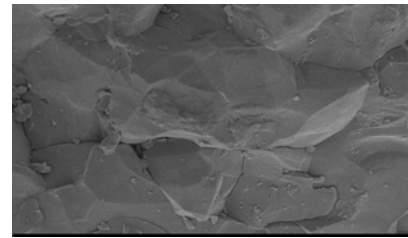
Table 1 Test scheme

Specimen label	Freeze-thaw cycle	Normal stress / MPa	Shear stress / MPa
S-1	0		
S-2	10		Initial: 2 MPa,
S-3	30	5	Loading level: 2 MPa,
S-4	50		Until failure
S-5	70		

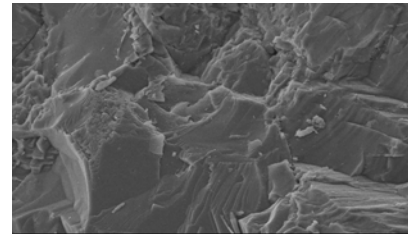
3 Analysis of meso-damage characteristics of freeze-thaw rocks

3.1 Scanning electron microscope test

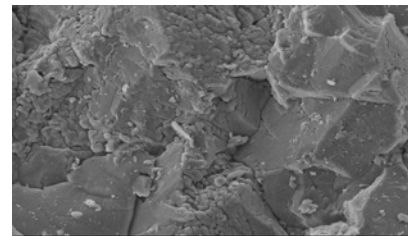
In order to reveal the effect of freeze-thaw cycles on the microstructure of granite, specimens subjected to different freeze-thaw cycles were analyzed by scanning electron microscope. Figure 5 shows the SEM images of specimens magnified 500 times under different freeze-thaw cycles.



(a) Frozen and thawed for 0 times



(b) Frozen and thawed for 30 times



(c) Frozen and thawed for 70 times

Fig.5 SEM images of samples under different freeze-thaw cycles

It is seen from Fig.5(a) that the surface of the specimen without being frozen and thawed is flat, the particles are closely arranged, the joints are not developed, and the pores are few. As the number of freeze-thaw cycles increases, the number of pores increases, the pore diameter increases, and some fine pores and microcracks begin to expand (see Fig. 5(b)). When the specimen was frozen and thawed for 70 times, the surface structure of the rock becomes loose and fragile, pores and fissures continue to develop, and the crack area gradually increases (see Fig. 5(c)). The test results indicate that with the increase of the number of freeze-thaw cycles, the pores and cracks of the specimen continue to develop and the damage of rock surface increases.

The EDS spectrum analysis was performed on the surface elements of the specimens. After normalizing all the elements, it was found that the surface elements of the granite were mainly Si and Al, and the content of K, O, Na, Al, Si, and Fe elements all show decreasing tendency with varying degrees after the freeze-thaw cycles. This is because of the alternation of cold and heat inside the rock, thermal expansion and contraction between the mineral particles lead to the loss of cementing elements between the particles.

3.2 Nuclear magnetic resonance test

Nuclear magnetic resonance technology was used to test the

specimens under different freeze-thaw cycles to obtain the variation of T_2 spectrum and porosity. Figure 6 shows the T_2 spectrum of specimens under different freeze-thaw cycles, it is seen that there are three peaks in the T_2 spectrum of the granite specimen, and the T_2 relaxation time is mainly distributed between 0.1 and 100 ms, which means the specimen is mainly composed of small and medium pores. When frozen and thawed for 0–30 times, the left-most peak increased significantly, and the remaining peaks changed slightly, indicating that the degree of freeze-thaw damage was low and only caused the development of micropores in the specimen. When frozen and thawed for 30–70 times, all the three peaks increase significantly, and the amplitude of the nuclear magnetic signal increases gradually, indicating that as the number of freeze-thaw cycles increases, the pores in the specimen begin to expand and the freeze-thaw damage increase.

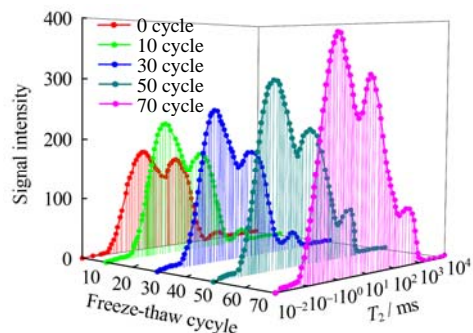


Fig.6 T_2 spectrum of samples under different freeze-thaw cycles

Figure 7 shows the variation of porosity of specimens under different freeze-thaw cycles. The porosity of the specimen shows a non-linear growth trend with the increase of the number of freeze-thaw cycles. The porosity increases slowly at 0–30 freeze-thaw cycles, while increases significantly at 30–70 freeze-thaw cycles. These results are basically consistent with the literature [18].

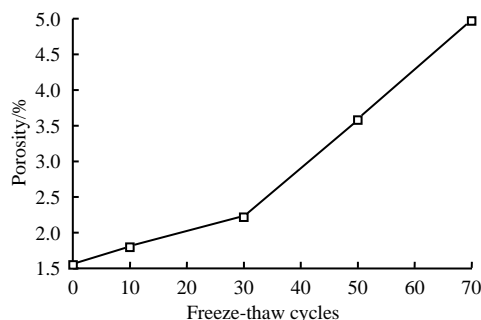


Fig.7 Porosity of samples under different freeze-thaw cycles

3.3 Analysis of freeze-thaw damage mechanism

The meso-damage characteristics of rocks after freeze-thaw

indicate that the freeze-thaw cycle promotes the development of surface and internal damage of the specimen, which is due to: (i) When the temperature drops to negative, the water in the cracks and pores of the specimen freeze into ice, resulting in continuous expansion of cracks and pores that promoted by the frost heaving force, and the rock will undergo frost heaving damage. As the temperature rises, the ice in the rock will melt into water, and the water will migrate into the newly generated cracks and pores. Greater frost heaving force will be produced by the freeze-thawing process, repeated in this way, ice-water phase change and water migration constantly cause deterioration of rock freeze-thaw damage. (ii) The expansion coefficient and shrinkage coefficient of mineral particles in the specimen are not consistent, resulting in new cracks caused by uneven deformation of rocks under freeze-thaw process. Cracks develop continuously and new cracks are generated under the action of frost heaving force, leading to gradual decrease of the friction and cementation between particles.

From the perspective of long-term stability of freeze-thaw rocks, the damage caused by freeze-thaw cycles affects the creep mechanical properties and parameters of rocks. Therefore, further research is needed through mechanical tests and mathematical models.

4 Analysis of shear creep test results

4.1 Effect of freeze-thaw cycles on creep deformation of specimens

Figure 8 shows the shear creep test curves of specimens under different freeze-thaw cycles, it is seen that the specimen has an instantaneous shear displacement immediately after the application of shear stress, and the instantaneous shear displacement gradually increases with the number of freeze-thaw cycles. Under long-term shear stress, the creep characteristics of the specimen are more obvious. As the shear stress increases, the creep displacement increases significantly, showing the characteristics of deceleration creep and stable creep. When applied to the last level of load, the specimens exhibit obvious accelerated creep characteristics, and the creep rate and creep displacement increase gradually with time, until they fail. With the increase of the number of freeze-thaw cycles, the shear displacement of the specimen increases gradually under the same load, and the creep curve gradually changes from gentle to steep.

It is seen from Table 2 that under the first-level load, the shear creep displacement of the sample with 0 freeze-thaw cycles is 0.188 5 mm. With the increase of the number of freeze-thaw cycles, the shear creep displacements of the freeze-thaw specimens with 10, 30, 50, 70 times are 0.270 9, 0.417 2, 0.528 7, 0.680 9 mm, respectively. This result indicates

that under the same load, as the number of freeze-thaw cycles increases, the damage caused by freeze-thaw will gradually increase the shear creep displacement of the specimen. After 30 freeze-thaw cycles, the shear creep displacement of the specimen under the first load is 0.417 2 mm. As the shear stress increases gradually, the shear creep displacement under the last load increases to 1.505 4 mm. Therefore, the shear creep displacement of the sample also increases accordingly with shear stress when under the same number of freeze-thaw cycles.

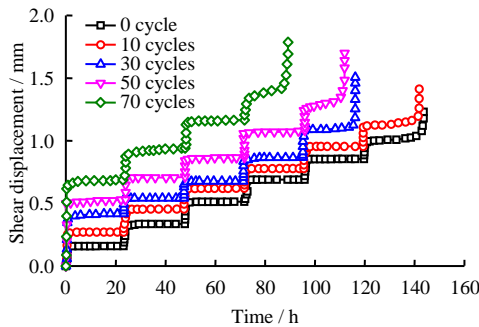


Fig.8 Shear creep curves of samples under different freeze-thaw cycles

Table 2 Shear creep deformation of samples under different shear stresses

Freeze-thaw cycle	Shear creep displacement under different shear stress(MPa)/mm					
	2	4	6	8	10	12
0	0.188 5	0.336 0	0.512 8	0.689 6	0.854 6	1.230 8
10	0.270 9	0.454 4	0.619 7	0.777 5	0.954 3	1.412 6
30	0.417 2	0.541 3	0.677 0	0.865 5	1.505 4	—
50	0.528 7	0.705 3	0.864 7	1.076 6	1.698 9	—
70	0.680 9	0.922 1	1.163 8	1.786 1	—	—

4.2 Effect of freeze-thaw cycles on creep rate of specimens

Figure 9 shows the relationship between shear steady-state creep rate and shear stress of granite under different freeze-thaw cycles. The shear steady-state creep rate of the specimen is not only affected by shear stress, but also closely related to the number of freeze-thaw cycles (see Fig.9). Under the same load, the shear steady-state creep rate of the specimen increases gradually with the number of freeze-thaw cycles. For example, under the first-level load, the shear steady-state creep rate of specimen under 0 freeze-thaw cycle is 1.48×10^{-5} mm/h. As the number of freeze-thaw cycle increases, the shear steady-state creep rates of specimens under 10, 30, 50, and 70 freeze-thaw cycles increase by 0.24×10^{-5} , 0.58×10^{-5} , 0.83×10^{-5} , and 1.26×10^{-5} mm/h, respectively, compared to the specimens under 0 freeze-thaw cycle. The shear steady-state creep rate of the specimen increases non-linearly with shear stress when under the same number of freeze-thaw cycles. The shear steady-state creep rate of the specimen under 10 freeze-thaw cycles increases from 1.72×10^{-5} mm/h when applied the first-

order load to 12.43×10^{-5} mm/h when applied the last-order load.

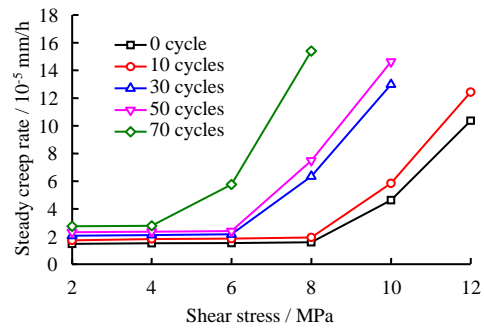


Fig.9 Shear steady creep rate curves of samples under different freeze-thaw cycles

Under the last stage load, the specimens have successively experienced the deceleration creep stage, the stable creep stage, and the accelerated creep stage, and rapid damage occurs during the accelerated creep stage. The relationship between the shear creep rate and time of the specimen is shown in Fig. 10. It is seen that the curve approximates a barrel shape, and the creep rate decreases firstly, then remains stable, and then increases suddenly.

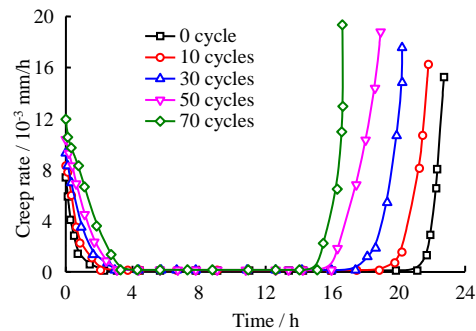


Fig.10 Shear creep rate curve of specimens under the last stage load

Table 3 shows the comparison of the stress levels, creep durations and creep rates of the specimens under different freeze-thaw cycles. The creep rate of the specimen increases with the number of freeze-thaw cycles. The initial creep rate, steady-state creep rate, and ultimate accelerated creep rate increase from $7.384 9 \times 10^{-3}$, 10.37×10^{-5} , $15.256 5 \times 10^{-3}$ mm/h under 0 freeze-thaw cycles to $11.948 3 \times 10^{-3}$, 15.39×10^{-5} , $19.342 6 \times 10^{-3}$ mm/h under 70 freeze-thaw cycles, respectively. As the number of freeze-thaw cycles increases, the creep time and failure stress of the specimen decrease gradually. Creep failure occurs at 12 MPa for specimens with 0 freeze-thaw cycles, and the creep time is 22.73 hours. With the increase of freeze-thaw cycles, the creep failure stress of the rock specimens under 10, 30, 50, and 70 freeze-thaw cycles are 12 MPa, 10 MPa, 10 MPa, and 8 MPa, respectively, and the creep duration are 21.79 h, 20.21 h, 18.92 h, and 16.62 h, respectively.

4.3 Effect of freeze-thaw cycles on the long-term strength of specimens

The long-term strength of the rock mass is an important indicator for the long-term stability and safety evaluation of rock mass engineering. The steady-state creep rate method is used to determine the long-term shear strength of the specimen^[19]. According to literature [20], the ratio of long-term shear strength to failure shear strength is defined as the long-term reduction coefficient. Due to space limitations, this paper only shows the relationship between the creep rate and the shear stress of the specimen under 10 freeze-thaw cycles (see Fig.11).

It is seen from Fig.11 that there is obvious inflection point in the curve. The tangents of the curve before and after the inflection point are plotted respectively, and the stress corresponding to the intersection point A is the long-term shear strength of the rock. According to this method, the long-term strengths of the specimens under 0, 10, 30, 50, and 70 freeze-thaw cycles are 11.18, 10.75, 8.61, 8.32, 6.23 MPa, respectively, and the long-term reduction coefficients are 0.932,

0.895, 0.861, 0.832, and 0.778, respectively. As shown in Fig.12, both the long-term shear strength and the long-term reduction coefficient of the specimens decrease gradually with the number of freeze-thaw cycles, indicating that the damage caused by the freeze-thaw cycles has a significant effect on the long-term strength of granite.

According to the analysis in Section 3, the freeze-thaw cycles cause damage to the surface and the interior of the specimen. In the creep test, under the long-term stress, these damaged cracks and pores have a more sufficient expansion time, the particle slip distance increases, and coarse particles edges or weak particles are more broken locally, resulting in continuous deterioration on the shear modulus, viscosity coefficient, and long-term strength of the sample. Therefore, as the number of freeze-thaw cycles increases, the creep time, failure stress and long-term strength of the specimen decrease gradually, while the creep deformation and creep rate increase gradually. In order to analyze the creep mechanism more deeply, a creep constitutive model is established in this paper.

Table 3 Creep parameters of samples under failure stress

Freeze-thaw cycle	Failure stress / MPa	Creep duration / h	Deceleration creep phase		
			Initial creep rate / (mm/h)	Steady creep rate / (mm/h)	Accelerated creep phase
					Ultimate accelerated creep rate / (mm/h)
0	12	22.73	7.3849×10^{-3}	10.37×10^{-5}	15.2565×10^{-3}
10	12	21.79	8.2992×10^{-3}	12.43×10^{-5}	16.2427×10^{-3}
30	10	20.21	9.2950×10^{-3}	12.98×10^{-5}	17.5441×10^{-3}
50	10	18.92	10.3738×10^{-3}	14.62×10^{-5}	18.7855×10^{-3}
70	8	16.62	11.9483×10^{-3}	15.39×10^{-5}	19.3426×10^{-3}

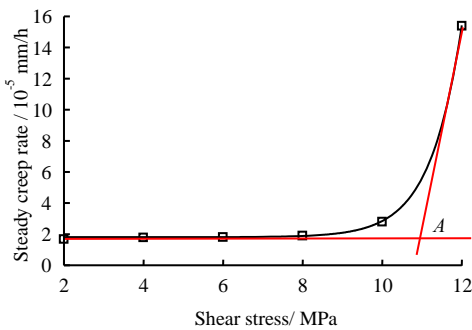


Fig.11 Creep rate-shear stress curve of samples under 10 freeze-thaw cycles

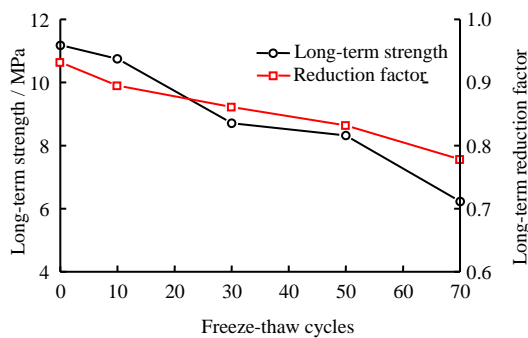


Fig.12 Long-term strength and reduction coefficient of samples under different freeze-thaw cycles

5 Granite shear creep model considering freeze-thaw effect

5.1 Expression of unsteady creep parameters for freeze-thaw rocks

The experimental results show that due to freeze-thaw cycles, cold and heat alternates with each other within the interior of the granite, resulting in expansion and contraction of mineral particles, which leads to deterioration of the rock mechanical properties. As the number of freeze-thaw cycles increases, the amount of creep deformation increases gradually and the creep rate accelerates significantly, while the creep time, failure stress and long-term strength all show a significant decrease. Therefore, the nonlinear aging characteristics of freeze-thaw rocks will be reflected more directly and objectively when treating rock rheological parameters as unsteady. This paper considers the effect of freeze-thaw cycles (n) on granite shear modulus G , viscosity coefficient η and other parameters to realize the expression of unsteady creep parameters for freeze-thaw rocks, i.e., $G = G(n)$, $\eta = \eta(n)$.

5.2 Damaged viscous elements for freeze-thaw rock

Previous studies have shown that damage will occur inside

the rock when the applied load reaches or exceeds a certain level of shear stress [21–22], so the effect of damage caused by shear stress on creep parameters should also be considered. This paper only considers the damage caused by the stress during the accelerated creep phase because of the relatively small damage caused by the stress during the deceleration creep phase and the steady creep phase.

As shown in Fig.13, the damaged viscous element under freeze-thaw conditions is constructed, considering the effect of freeze-thaw cycles, and the damage variable D is introduced to describe the damage degradation of the viscosity coefficient of the specimen during the accelerated creep stage.

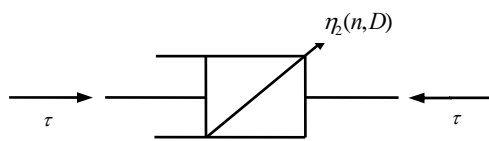


Fig.13 Damaged viscous elements under freeze-thaw conditions

According to Newton's law of viscosity, the constitutive relation of damaged viscous elements under freeze-thaw conditions is given by

$$\tau = \eta_2(n,D)\dot{\gamma} \tag{1}$$

where τ and $\dot{\gamma}$ are the shear stress and shear strain rate of damaged viscous elements under freeze-thaw conditions, respectively; $\eta_2(n,D)$ is the viscosity coefficient of damaged viscous elements under freeze-thaw conditions. Considering the effects of freeze-thaw cycles and stress time on the viscosity coefficient, the $\eta_2(n,D)$ can be expressed as

$$\eta_2(n,D) = \eta_2(n)(1 - D) \tag{2}$$

where $\eta_2(n)$ is the viscosity coefficient under n freeze-thaw cycles; D is the damage variable, $0 \leq D < 1$.

The damage variable and time have a negative exponential function relationship during rock creep [23–24], i.e.:

$$D = 1 - e^{-\alpha t} \tag{3}$$

where α is a coefficient related to the number of freeze-thaw cycles; t is time. Therefore, Eq. (2) transformed to

$$\eta_2(n,D) = \eta_2(n)e^{-\alpha(n)t} \tag{4}$$

Keeping the stress constant and combining Eqs. (1) and (4), the constitutive relationship of the damaged viscous elements under freeze-thaw conditions is given by

$$\dot{\gamma}(t) = \frac{\tau}{\alpha(n)\eta_2(n)} [e^{\alpha(n)t} - 1] \tag{5}$$

5.3 Shear creep model of freeze-thaw rock

Experimental results reveal that the granite has experienced deceleration creep stage, stable creep stage, and accelerated

creep stage under freeze-thaw cycles. The classic Nishihara model can well describe the deceleration creep and steady-state creep phases in rock creep tests, but it cannot reflect the accelerated creep characteristics of rocks. Therefore, based on the Nishihara model, the viscous elements in the viscoplastic body are replaced by freeze-thaw damaged viscous elements, and a freeze-thaw shear creep constitutive model for granite is established considering the effects of freeze-thaw cycles on model parameters (see Fig. 14). The model is composed of a freeze-thaw elastic element, a freeze-thaw viscoelastic body, and a freeze-thaw damaged viscoplastic body, and the shear strains are γ_0 , γ_1 , and γ_2 , respectively.

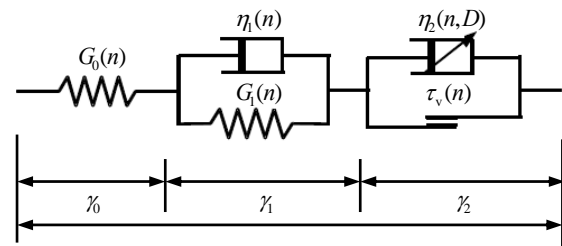


Fig.14 Constitutive model of freeze-thaw shear creep

The total shear stress is τ , and the total shear strain γ can be expressed as

$$\gamma = \gamma_0 + \gamma_1 + \gamma_2 \tag{6}$$

The stress-strain relationship for the freeze-thaw elastic element is given as

$$\gamma_0 = \frac{\tau}{G_0(n)} \tag{7}$$

where $G_0(n)$ is the shear modulus of the freeze-thaw elastic element under n freeze-thaw cycles.

Freeze-thaw viscoelastic body is composed of freeze-thaw elastic element and freeze-thaw viscous element in parallel. The constitutive relationship of the freeze-thaw viscous element is given by

$$\tau_H = \eta_1(n)\dot{\gamma}_H \tag{8}$$

where τ_H and γ_H are the shear stress and shear strain of freeze-thaw viscous element, respectively; $\eta_1(n)$ is the viscosity coefficient of freeze-thaw viscous element under n freeze-thaw cycles.

Therefore, according to the combined model theory, the stress-strain relationship of freeze-thaw viscous element is expressed as

$$\left. \begin{aligned} \gamma_1 &= \gamma_H = \gamma_K \\ \tau &= \tau_H + \tau_K = \eta_1(n)\dot{\gamma}_H + G_1(n)\gamma_K \end{aligned} \right\} \tag{9}$$

where γ_K and $G_1(n)$ are shear strain and shear modulus of freeze-thaw viscous element, respectively. Combining with the initial conditions $t = 0$, Eq. (9) can be solved as

$$\gamma_1 = \frac{\tau}{G_1(n)} \left(1 - e^{-\frac{G_1(n)t}{\eta_1(n)}} \right) \quad (10)$$

Freeze-thaw viscoplastic body is composed of freeze-thaw plastic element and freeze-thaw viscous element in parallel. The shear stress of plastic element τ_v can be expressed as

$$\tau_v = \begin{cases} \tau, \tau < \tau_s \\ \tau_s, \tau \geq \tau_s \end{cases} \quad (11)$$

where τ_s is the yield stress.

According to the combined model theory, the relationship is given by

$$\tau = \tau_D + \tau_v \quad (12)$$

where τ_D is the stress of freeze-thaw damaged viscous element.

When $\tau < \tau_s$, combining Eqs. (11) and (12), the relationship can be solved as $\tau_D = 0$, i.e., $\gamma_2 = 0$.

When $\tau \geq \tau_s$, combining the constitutive relationship of freeze-thaw damaged viscous element, the relationship can be solved as

$$\gamma_2 = \frac{\tau}{\alpha(n)\eta_2(n)} [e^{\alpha(n)t} - 1] \quad (13)$$

hence:

$$\gamma_2 = \begin{cases} 0, \tau < \tau_s \\ \frac{\tau - \tau_s}{\alpha(n)\eta_2(n)} [e^{\alpha(n)t} - 1], \tau \geq \tau_s \end{cases} \quad (14)$$

Considering the strains of freeze-thaw elastic element, freeze-thaw viscoelastic body and freeze-thaw damaged viscoplastic body, the constitutive equation of freeze-thaw shear creep model of granite can be expressed as

$$\gamma(t) = \begin{cases} \frac{\tau}{G_0(n)} + \frac{\tau}{G_1(n)} \left(1 - e^{-\frac{G_1(n)t}{\eta_1(n)}} \right), \tau < \tau_s \\ \frac{\tau}{G_0(n)} + \frac{\tau}{G_1(n)} \left(1 - e^{-\frac{G_1(n)t}{\eta_1(n)}} \right) + \frac{\tau}{\alpha(n)\eta_2(n)} [e^{\alpha(n)t} - 1], \tau \geq \tau_s \end{cases} \quad (15)$$

5.4 Parameter identification and model verification

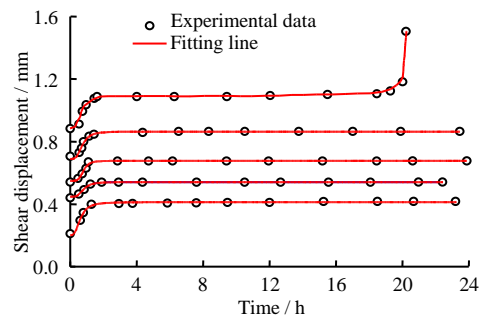
The Boltzmann superposition principle is used to convert the creep curve under the gradation loading condition to the creep curve under the separate loading condition. Based on the experimental results, the model parameters are identified using 1stOpt mathematical optimization analysis software. Due to space limitations, only the creep parameter identification results of specimens under 30 and 70 freeze-thaw cycles are listed in Table 4.

Table 4 Parameters of freeze-thaw shear creep model

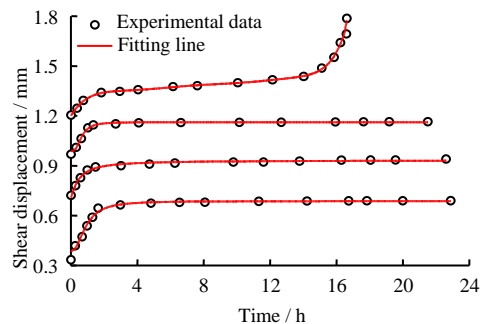
Freeze-thaw cycle	Shear stress / MPa	G_0 / GPa	G_1 / GPa	η_1 / (GPa·h)	η_2 / (GPa·h)	α
30	2	25.56	2.03	89.66	—	—
	4	17.59	1.74	62.73	—	—
	6	12.46	1.63	46.59	—	—
	8	9.62	1.45	28.34	—	—
	10	6.24	1.13	10.75	212.52	0.61
70	2	15.48	1.54	47.52	—	—
	4	11.59	1.27	30.48	—	—
	6	7.47	1.01	17.54	—	—
	8	3.79	0.72	5.54	82.29	0.90

Figure 15 shows the comparison between the creep test curve and the theoretical model fitting curve for the specimens under 30 and 70 freeze-thaw cycles. It is seen that the two curves agree well, and the model fitting curve can well reflect the deceleration creep, stable creep, and accelerated creep characteristics of granite under different freeze-thaw cycles, indicating the correctness and applicability of the freeze-thaw shear creep constitutive model established in this paper.

A sensitivity analysis of the creep parameters η_2 and α for damaged freeze-thaw viscous elements is conducted to study their effects on the creep deformation of granite, the other parameters are selected from the values of the specimens under 70 freeze-thaw cycles and with a shear stress of 8 MPa that listed in Table 4.



(a) Frozen and thawed for 30 times



(b) Frozen and thawed for 70 times

Fig.15 Comparison of test data with fitting curve

Figures 16 and 17 show the influences of the creep parameters η_2 and α on the creep deformation curves, respectively. It is seen from Fig.16 that when the other parameters remain unchanged, the steady-state creep rate and creep deformation of the rock gradually decrease and the steady-state creep time increases as the viscosity coefficient η_2 increases. It is seen from Fig. 17 that when the other parameters remain unchanged, with the increase of the creep parameters α , the creep rate and creep deformation of the accelerated stage of the rock gradually increase while the failure time decreases, and the transition from viscoelastic to viscoelastic-plastic of rock becomes easier.

5.5 Variation of model parameters with the number of freeze-thaw cycles

According to the fitting results of shear moduli G_0 and G_1 , and viscosity coefficients η_1 and η_2 , and α in the freeze-thaw shear creep model of granite, the average values are respectively taken to obtain the relationship between each parameter and the number of freeze-thaw cycles, which is given by

$$\left. \begin{aligned} G_0(n) &= 18.9055e^{-0.0099n}, R^2 = 0.99056 \\ G_1(n) &= 1.9540e^{-0.0078n}, R^2 = 0.98525 \\ \eta_1(n) &= -0.5857n + 65.436, R^2 = 0.98016 \\ \eta_2(n) &= 381.954e^{-0.0224n}, R^2 = 0.98642 \\ \alpha(n) &= 0.0084n + 0.3507, R^2 = 0.98908 \end{aligned} \right\} \quad (16)$$

Figure 18 shows the fitting curves of various parameters of the granite freeze-thaw shear creep model with the number of freeze-thaw cycles (n). The shear moduli G_0 and G_1 , and viscosity coefficient η_2 all decrease gradually with the increase of the number of freeze-thaw cycles, which are in line with the exponential function. The variation of viscosity coefficients (η_1 and α) with the number of freeze-thaw cycles conforms to a linear function. As the number of freeze-thaw cycles increases, η_1 decreases, and α increases. On the other hand, changes in model parameters will cause the creep deformation and creep rate to increase gradually with the number of freeze-thaw cycles, which is also consistent with the experimental results.

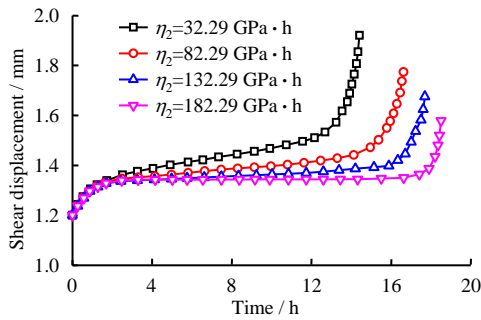


Fig.16 Effect of creep parameter η_2 on shear creep curves

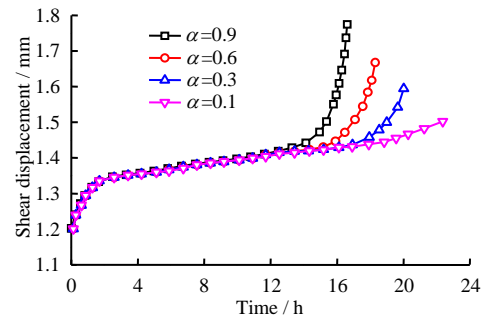
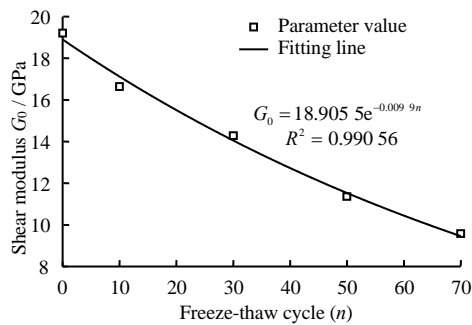
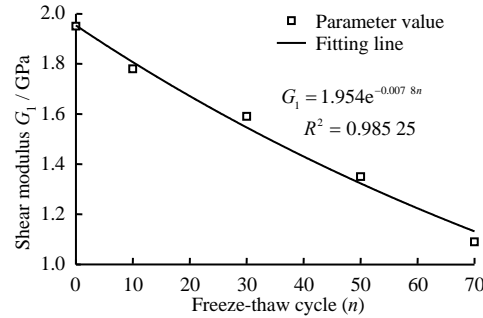


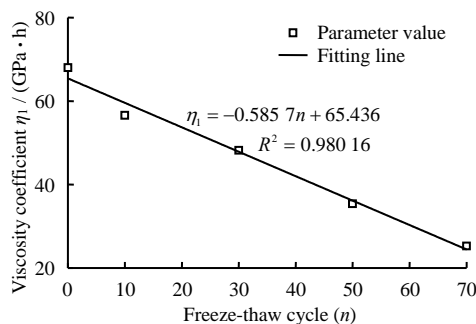
Fig.17 Effect of creep parameter α on shear creep curve



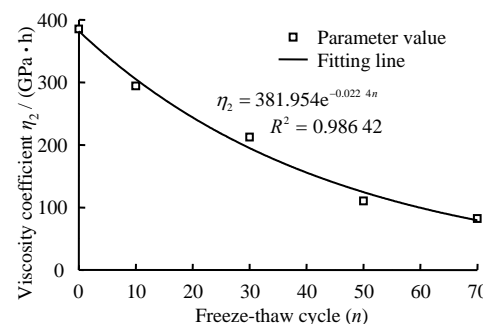
(a) Fitting line of relationship between G_0 and freeze-thaw cycle



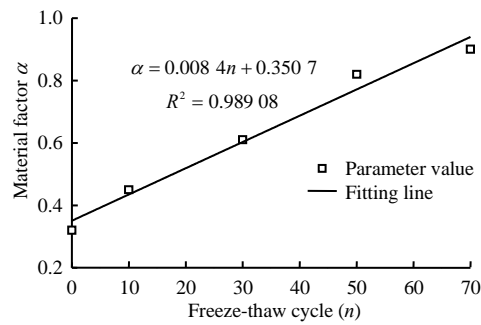
(b) Fitting line of relationship between G_1 and freeze-thaw cycle



(c) Fitting line of relationship between η_1 and freeze-thaw cycle



(d) Fitting line of relationship between η_2 and freeze-thaw cycle

(e) Fitting line of relationship between α and freeze-thaw cycle**Fig.18** Variation in the curves of creep parameters of granite with the freeze-thaw cycles

6 Conclusions

The effects of freeze-thaw cycles on the microstructure of granite were studied by scanning electron microscope and nuclear magnetic resonance experiments. As the number of freeze-thaw cycles increases, the cracks and pores in the specimens continue to develop and evolve, and the surface damage of the rock becomes more and more obvious. The pores in the specimens are mainly small and medium, and the porosity increases non-linearly with the number of freeze-thaw cycles. Porosity increases slowly at 0–30 freeze-thaw cycles, and increases significantly at 30–70 freeze-thaw cycles.

Freeze-thaw cycles have a great influence on the creep mechanical properties of granite. As the number of freeze-thaw cycles increases, the amount of creep deformation and creep rate gradually increase, while the creep duration, failure stress and long-term strength all show a significant decrease. These results indicate that the freeze-thaw cycle promotes the development of specimen damage, resulting in continuous deterioration on the mechanical properties and creep parameters of the specimen.

Considering the effects of freeze-thaw cycles on the model parameters, this paper proposes a damaged freeze-thaw viscous element for rock and establishes a constitutive model for freeze-thaw shear creep of granite. This model can well reflect the deceleration creep, stable creep and accelerated creep characteristics of granite under different freeze-thaw cycles.

According to the experimental results, the parameters in the model were identified, and the creep test curve was compared with the curve fitted by the theoretical model to verify the correctness and applicability of the model. The sensitivity analysis of the creep parameters reveals their influences on the creep deformation of the granite, and the change law of the creep parameters with the number of freeze-thaw cycles is given.

References

[1] SUN Jun. Rock rheological mechanics and its advance in

engineering applications[J]. Chinese Journal of Rock Mechanics and Engineering, 2007, 26(6): 1081–1106.

- [2] JIA C, XU W, WANG R, et al. Experimental investigation on shear creep properties of undisturbed rock discontinuity in Baihetan hydropower station[J]. International Journal of Rock Mechanics and Mining Sciences, 2018, 104: 27–33.
- [3] ZHAO H, ZHANG H, LI H, et al. Formation and fractal characteristics of main fracture surface of red sandstone under restrictive shear creep[J]. International Journal of Rock Mechanics and Mining Sciences, 2017, 98: 181–190.
- [4] ZHANG Q, SHEN M, DING W. The shear creep characteristics of a Green Schist weak structural marble surface[J]. Mechanics of Advanced Materials and Structures, 2015, 22(9): 697–704.
- [5] XU T, XU Q, RANJITH P G. The evolution of rock failure with discontinuities due to shear creep[J]. Acta Geotechnica, 2013, 8(6): 567–581.
- [6] SUN Jun, LI Yong-sheng, LI Xiang-sheng. The rheological characteristics of tunnel opening in multi-set joint rock mass and its viscous elastoplastic effects[R]. Shanghai: Tongji University, 1984.
- [7] WANG Zhen, SHEN Ming-rong, TIAN Guang-hui, et al. Time-dependent strength of rock mass discontinuity with different values of JRC[J]. Chinese Journal of Rock Mechanics and Engineering, 2017, 36(Suppl.1): 3287–3296.
- [8] TIAN Guang-hui, SHEN Ming-rong, ZHANG Qing-zhao, et al. Study on shear creep, relaxation and long term strength of serrate structure surface[J]. Journal of Harbin Institute of Technology, 2018, 50(6): 120–129.
- [9] XU Wei-ya, YANG Sheng-qi. Experiment and modeling investigation on shear rheological property of joint

- rock[J]. *Chinese Journal of Rock Mechanics and Engineering*, 2005, 24(Suppl.2): 264–270.
- [10] YANG Sheng-qi, NI Hong-mei. A viscoelastic shear creep model of mudstone: parameter identification[J]. *Journal of China University of Mining & Technology*, 2012, 41(4): 551–557.
- [11] LI Peng, LIU Jian, ZHU Jie-bing, et al. Research on effects of water content on shear creep behavior of weak structural plane of sandstone[J]. *Rock and Soil Mechanics*, 2008, 29(7): 1865–1871.
- [12] YU Yong-jiang, ZHANG Wei, ZHANG Guo-ning, et al. Study of nonlinear shear creep model and creep property experiment of water-rich soft rock[J]. *Journal of China Coal Society*, 2018, 43(6): 1780–1788.
- [13] LIU Xue-zeng, SU Jing-wei, WANG Xiao-xing. Experimental investigation on shear rheological properties of tufflava with different grades[J]. *Chinese Journal of Rock Mechanics and Engineering*, 2009, 28(1): 190–197.
- [14] FAN Qiu-yan, ZHANG Bo, LI Xian. Experimental research on shear creep properties of a swelling rock under different expansive states[J]. *Chinese Journal of Rock Mechanics and Engineering*, 2016, 35(Suppl.2): 3734–3746.
- [15] LI Zhi-jing, ZHU Zhen-de, ZHU Ming-li, et al. Study on shear creep and roughness effect on hard discontinuities of marble[J]. *Chinese Journal of Rock Mechanics and Engineering*, 2009, 28(Suppl.1): 2605–2611.
- [16] ZHU Zhen-de, LI Zhi-jing, ZHU Ming-li, et al. Shear rheological experiment on rock mass discontinuities and back analysis of model parameters[J]. *Rock and Soil Mechanics*, 2009, 30(1): 99–104.
- [17] CCCC Second Highway Consultants Co., Ltd. JTG E41 — 2005 Tests methods of rock for highway engineering[S]. Beijing: China Communications Press, 2005.
- [18] YANG Geng-she, SHEN Yan-jun, JIA Hai-liang, et al. Research progress and tendency in characteristics of multi-scale damage mechanics of rock under freezing-thawing[J]. *Chinese Journal of Rock Mechanics and Engineering*, 2018, 37(3): 545–563.
- [19] MA Qin-yong, YU Pei-yang, YUAN Pu. Experimental study on creep properties of deep siltstone under cyclic wetting and drying[J]. *Chinese Journal of Rock Mechanics and Engineering*, 2018, 37(3): 593–600.
- [20] CHEN Guo-qing, GUO Fan, WANG Jian-chao, et al. Experimental study of creep properties of quartz sandstone after freezing-thawing cycles[J]. *Rock and Soil Mechanics*, 2017, 38(Suppl.1): 203–210.
- [21] WANG Chun-ping, CHEN Liang, LIANG Jia-wei, et al. Creep constitutive model for full creep process of granite considering thermal effect[J]. *Rock and Soil Mechanics*, 2014, 35(9): 2494–2500.
- [22] SHAN Ren-liang, SONG Li-wei, LI Dong-yang, et al. Study of nonlinear creep model of frozen red sandstone[J]. *Rock and Soil Mechanics*, 2014, 35(6): 1541–1546.
- [23] CAI Ting-ting, FENG Zeng-chao, ZHAO Dong, et al. A creep model for lean coal based on hardening-damage mechanism[J]. *Rock and Soil Mechanics*, 2018, 39(Suppl.1): 61–68.
- [24] CAI Yu, CAO Ping. A non-stationary model for rock creep considering damage based on Burgers model[J]. *Rock and Soil Mechanics*, 2016, 37(Suppl.2): 369–374.